Viscous gravity currents inside confining channels and fractures

Daisuke Takagi and Herbert E. Huppert
Institute of Theoretical Geophysics, University of Cambridge, Wilberforce Road,
Cambridge CB3 0WA, United Kingdom

Unidirectional flows of long, thin, Newtonian, viscous gravity currents inside either horizontal or inclined channels are studied theoretically and experimentally. Effects due to temporal variations in the input rate at a point source and spatial variations in the channel shape are considered, with surface tension effects neglected. The current evolves with a self-similar structure at large times when the total volume of fluid scales with time t like t^{α} and the spreading in the lateral direction y is constrained by a rigid boundary of height $a|y/a|^{n}$, where the length scale of the channel size a varies with distance x along the flow like x^{b} and $\alpha \geq 0$, $b \geq 0$ and $n > 0$ are prescribed constants. The extent of the flow scales like t^{c}, where the constant c depends linearly on α and is determined in terms of α, b, and n. Amongst channels that remain uniform along the flow ($b=0$), a V-shaped channel ($n=1$) gives rise to either a fastest or slowest propagation rate of the current depending on whether $\alpha < \alpha_c$ or $\alpha > \alpha_c$, respectively, while the value of c is the same for all n when $\alpha = \alpha_c$, with either $\alpha_c = 1/2$ or $\alpha_c = 1$ for horizontal or inclined flows, respectively. The position of a current inside either an extremely narrow or nearly flat V-shaped channel that gently widens along the flow is also studied and shown to be proportional to a power of time. We determine that the spreading is constrained mainly by volume conservation for the case $n > 1$ inside wide channels and by frictional drag at the rigid boundaries for $n < 1$ inside narrow fractures. © *2008 American Institute of Physics*.
[DOI: 10.1063/1.2883991]

I. INTRODUCTION

Low-Reynolds-number gravity currents occur when a viscous fluid propagates slowly horizontally or down a slope into an ambient fluid of a different density. An everyday example is honey spreading over toast. Examples in nature include lava flows on land[1,2] and lithospheric materials spreading inside the Earth's mantle.[3] In industry, glass spreading in melting glass furnaces[4] plays an important role in the manufacturing process. The main feature of all these currents is that the motion is governed by a balance between forces due to viscosity and gravity. Effects due to inertia are negligible to leading order.[5,6]

When a Newtonian fluid is released from a point source onto a dry rigid surface, a thin layer can quickly develop and slowly spread as a viscous gravity current at longer times. The resulting Stokes flow with negligible surface tension effects often evolves with a self-similar structure, which means that regardless of the initial configurations, the position of the front scales with time like t^{c} for some c that depends on the geometry of the underlying rigid surfaces and the input rate at the source. In the case of releasing a fixed volume of fluid, the value of the exponent c is $1/8$ for axisymmetric spreading over an impermeable horizontal plane,[5] $1/3$ for spreading down a flat incline,[7,8] $1/4$ and $2/7$ for spreading inside cylindrical and V-shaped channels along a horizontal, and $3/7$ and $1/2$ down sloping cylindrical and V-shaped channels, respectively.[9] Laboratory experiments on a flat incline show, in addition, that either a series of small amplitude waves or a single capillary rivulet develops at the front and produces extended regions thereafter when the current is ini-

tiated from a line[7] or point source,[8] respectively. This is due to surface tension effects that eventually influence the ever thinning flow front. Such instabilities, however, have not yet been observed in any of the experiments inside sloping semi-circular or V-shaped channels.[9]

The theoretical framework for studying Stokes flows forms an important foundation for considering additional factors that influence the flow of viscous gravity currents. In modelling the spreading of basaltic lava on land, for example, the formation of levees and channelized flows have been studied based on the assumption that the current evolves like a Stokes flow initially near the vent.[10] Newtonian results have formed a basis for comparison in studying the effects due to compressibility of lava as a result of bubbles forming inside,[11] surface cooling[12] and solidification as a result of forming a crustal boundary layer.[13] Where non-Newtonian effects play an important role, various different stress-strain relationships are considered in the study of viscous gravity currents with a Bingham[14,15] or a power-law rheology.[16,17]

The current paper extends previous work on Stokes flows in confining channels,[9] which considered an instantaneous fixed-volume release in channels with uniform cross section and found the resultant flows to evolve in a self-similar structure. In this paper, we consider the fluid volume to be time dependent and the channel shape to vary gently with distance from the source. One of the motivations of the research is to provide the foundations for studying lava flows, which are influenced by temporarily varying effusion rates and guided by valleys that narrow or widen in places.[18,19] The aim is to analyze the temporal behavior of

the position of the front as a consequence of either temporal variations in the input rate of fluid at the point source or spatial variations in the confining boundaries.

We derive the governing equations in Sec. II A by considering the total volume of fluid to vary with time like t^{α} inside an arbitrary channel, where α is a prescribed constant. When the channel is resting on a horizontal or inclined plane and its height is given by $d=a|y/a|^n$ for some $n>0$, where y is the coordinate in the lateral direction and a is the length scale of the channel size that scales with distance x along the flow as x^b for some given b, the structure of the resultant current is shown to evolve in a self-similar form. The mathematical solutions are presented for propagation inside wide channels $(n>1)$ in Sec. II B and inside narrow fractures $(n<1)$ in Sec. II C. When $n=1$, or more specifically when the channel height is given by $d=|y|/m$ and m increases like x^b, which corresponds to a gently widening V-shaped channel, the structure of the flow is only self-similar in special cases for general $b>0$ and is studied in Sec. II D.

Where self-similar solutions exist, the parameter c increases linearly with α and generally decreases with increasing b, which corresponds to further widening of wide channels or squeezing of narrow fractures. This indicates that the flow slows down in gently widening channels due to the constraints of volume conservation and also in gently squeezing fractures due to the rise in frictional drag at the boundaries. We determine amongst channels that remain uniform in cross section $(b=0)$ that c is independent of n in the special case of $\alpha=\alpha_c$ for some α_c, and it attains either a maximal or minimal value when $n=1$ in the case of $\alpha<\alpha_c$ or $\alpha>\alpha_c$, respectively. This critical value α_c is given by $\alpha_c=1/2$ when the flow is horizontal or $\alpha_c=1$ down an incline. Experimental data are in good agreement with the theoretical results and are presented for a constant flux $(\alpha=1)$ of glycerine that partially fills and spreads along either a horizontal or inclined channel with either a cylindrical $(n=2)$ or V-shaped $(n=1)$ boundary in Sec. III. Finally, in Sec. IV, we summarize the variety of qualitative and quantitative behavior of viscous gravity currents that arise inside different channels.

II. THEORY

A. Formulation

Consider an incompressible Newtonian fluid of constant density ρ and dynamic viscosity μ released onto a rigid channel, resting on a plane inclined at an angle θ to the horizontal. We adopt a Cartesian set of axes, where x denotes the downslope coordinate measured from the point of release, y the cross-slope coordinate, and z the coordinate normal to the plane. The height of the rigid confining boundary is denoted by $d(x,y)$.

Consider the regime after sufficient time t from initiation, where the fluid occupies the local width of the channel and spreads essentially in the x direction only. Any variation in the height of the current across the channel would lead to a cross-stream pressure gradient and a flow which reduces that height differential. Thus we can consider the height of the current to be uniform across the channel, and given by
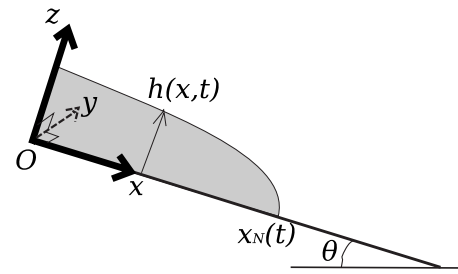

FIG. 1. A sketch of the current in the (x,z)-plane.

$h(x,t)$, dependent only on x and t as shown in Fig. 1. While the extent of the flow $x_N(t)$ is much greater than both this thickness and the fluid width, only the x-component of the velocity profile is nonzero and denoted by $u(x,y,z,t)$, where $\partial/\partial x \ll \partial/\partial y, \partial/\partial z$. With the assumption that effects due to surface tension are negligible, the fluid pressure is given by

$$p = p_0 + \rho g[(h-z)\cos\theta - x\sin\theta], \tag{1}$$

where p_0 is the constant reference pressure and g is gravity. A current under a deep layer of ambient fluid of density $\rho_a<\rho$ can be described by replacing g in Eq. (1) with the reduced gravity $g(\rho-\rho_a)/\rho$ because the stress exerted by the ambient fluid on the current is negligible.[5]

The velocity profile satisfies the Stokes equation

$$\mu\nabla^2 u = \frac{dp}{dx}, \tag{2}$$

where ∇ denotes the gradient operator in the (y,z)-plane. The dominant term on the right-hand side of Eq. (2) is
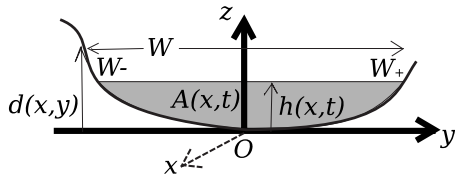
$$\frac{dp}{dx} = \rho g \sin^{1-H}\theta[-(\partial h/\partial x)]^H, \tag{3}$$

where H takes the value 1 for horizontal flows $\theta=0$ and 0 for flows down a slope sufficiently inclined so that $\tan\theta \gg \partial h/\partial x$. This indicates that u is linear in either $-\partial h/\partial x$ or $\sin\theta$, depending on whether the flow is horizontal and driven by the slope of the free surface or inclined and driven by the component of gravity down the slope. An exact solution for u can be found in either case by specifying two associated boundary conditions. One is the no-slip condition $u=0$ at the rigid boundary $z=d$. The other is at the free surface $z=h$, where the shear stress is negligible and hence $\partial u/\partial z=0$ there. Different velocity profiles arise inside channels of different shapes and are treated separately for $n>1$, $n<1$, $n=1$ in Secs. II B–II D, respectively.

The velocity profile u is substituted into the definition of the downstream volume flux at any distance x from the source in the form

$$Q(x,t) = \int_A u\,dA, \tag{4}$$

where the integral is evaluated over the cross-sectional area of the fluid

FIG. 2. A sketch of the current in the (y,z)-plane.

FIG. 3. A cross section of the boundary $d=a|y/a|^n$ in the (y,z) plane with various different values of n, where the shaded region is a thin layer of fluid for the case $n=2$.

$$A(x,t) = \int_{W_-}^{W_+} dy \int_d^h dz \tag{5}$$

and $W=W_+ - W_-$ is the width of the current, with W_- and W_+ the y coordinates of the two points where the free surface h is in contact with the rigid boundary d, as sketched in Fig. 2. An expression for the volume flux Q, which has the right-hand side of Eq. (3) as a multiplicative factor, can be determined exactly in terms of the unknown height h wherever the boundary d is given.

The problem is formulated completely by the depth-averaged equation of continuity[20]

$$\frac{\partial A}{\partial t} + \frac{\partial Q}{\partial x} = 0, \tag{6}$$

the constraint on the total volume

$$\int_0^{x_N(t)} A\,dx = qt^\alpha, \tag{7}$$

where q and α are given numerical constants with $\alpha=0$ corresponding to the instantaneous release of a constant volume of fluid, and the condition

$$h[x_N(t),t] = 0, \tag{8}$$

which requires that the height of the current vanishes at the front. This final condition (8) is not satisfied by our model when the flow is inclined ($H=0$), for which the order of the equation governing the main structure of the current Eq. (6) is lower. In this case, a frontal region dominated by surface tension brings the height of the flow down to zero. We neglect this small region which does not influence the rate of propagation of the current or its shape, except at the front.[7]

Solutions for the unknowns h and x_N can be obtained using similarity variables[21] when Eqs. (6) and (7) are of the form

$$x^{e_1}\frac{\partial h^{e_2}}{\partial t} + G\frac{\partial}{\partial x}\left[x^{e_3}h^{e_4}\left(-\frac{\partial h}{\partial x}\right)^H\right] = 0 \tag{9}$$

and

$$\int_0^{x_N(t)} x^{e_1}h^{e_2}dx = \bar{q}t^\alpha, \tag{10}$$

where e_1, e_2, e_3, e_4, G, and $\bar{q}$ are independent of x and t and take various different values depending on the channel shape, as we explore in the next subsections. By considering the scaling factors in Eqs. (9) and (10), the scaling laws for x and h are given by
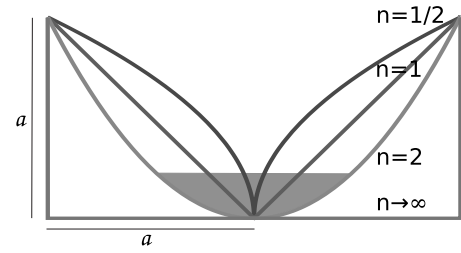
$$x \sim [G^{E_2}\bar{q}^{E_4}t^{\alpha E_4 + E_2}]^{1/E} \tag{11}$$

and

$$h \sim [G^{-E_1}\bar{q}^{E_3}t^{\alpha E_3 - E_1}]^{1/E} \tag{12}$$

with $E_1 = e_1 + 1$, $E_2 = e_2$, $E_3 = -e_3 + e_1 + 1 + H$, $E_4 = e_4 + H - e_2$, and $E = e_4 + e_1 e_4 - e_2 e_3 + H(1 + e_1 + e_2)$. It follows that the position of the front of the current x_N scales like Eq. (11) and is given by

$$x_N(t) = \eta_N G^{E_2/E}\bar{q}^{E_4/E}t^c, \tag{13}$$

where the constants $c = (\alpha E_4 + E_2)/E$ and η_N, a dimensionless number, depend on α, H, and the shape of the channel. An analytic expression for η_N can be obtained in the case $\alpha=0$ of a constant-volume release at the source by firstly obtaining an analytic solution for h with some steps of algebra, which are presented in the Appendix. For general $\alpha>0$, however, we must resort to a numerical scheme to determine η_N, which is also outlined in the Appendix. In the next subsections, we explore how different values of c and η_N arise by considering flows inside different channels.

B. Widening channels

Consider a channel described by the general power-law relationship $d=a|y/a|^n$, where a is the length scale associated with the channel width and $n>1$ is fixed so that the flow remains thin, wide, and very long at large times. A thin flow inside a cylindrical surface with a radius of curvature of $a/2$ is described by $n=2$ and inside a rectangular channel of width $2a$ with negligible effects due to the presence of lateral walls by $n\to\infty$, which is equivalent to two-dimensional flows along a flat surface (Fig. 3). It must be stressed here that the current only occupies a small depth $h\ll a$. The essential feature inside all these channels is that the depth of the current is much smaller than its width, so by the lubrication approximation, $\partial/\partial y \ll \partial/\partial z$, in which limit Eq. (2) becomes an ordinary second-order differential equation in u. The velocity profile determined to satisfy the boundary conditions is parabolic and given by

$$u = \frac{1}{2\mu}\frac{dp}{dx}(z-d)(2h-z-d) \tag{14}$$

with dp/dx given by Eq. (3).

Suppose the length scale of the channel width is given by $a=rx^b$ for some fixed values of r and b, so that special
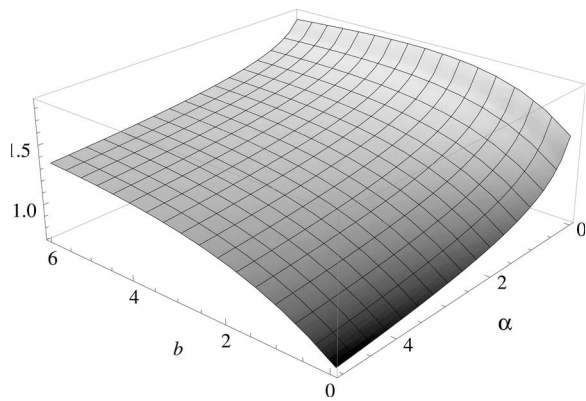
FIG. 4. Surface plot of η_N as a function of α and b in the case of horizontal flow $H=1$ with channel shape $n=2$.

cases of a channel that either remains uniform or varies linearly in width along the flow are represented by $b=0$ or $b=1$, respectively. By substituting Eq. (14) into Eq. (4), evaluating the integrals (4) and (5) and substituting them into the evolution Eq. (6), we obtain Eqs. (9) and (10), where the coefficients are $G=2g\sin^{1-H}\theta n^2/[\nu(2n+1)(3n+1)]$ and $\bar{q}=qr^{1/n-1}(n+1)/(2n)$ and the exponents are $e_1=e_3=b(1-l)$, $e_2=1+l$, $e_4=3+l$ with $l=1/n$. The position of the front of the current is given by Eq. (13), where

$$c=\frac{1+n+\alpha n(2+H)}{n+(2n+1)(1+H)+b(n-1)(2+H)} \quad (15)$$

and the dimensionless number η_N depends on α, b, n, and H. By considering all partial derivatives of Eq. (15), we determine for flows inside channels with a uniform cross section ($b=0$) that c is a strictly decreasing function of n for $\alpha<\alpha_c$ and increasing function of n for $\alpha>\alpha_c$, where α_c is a critical value given by either $\alpha_c=1/2$ in the horizontal case ($H=1$) or $\alpha_c=1$ in the inclined case ($H=0$). When a fluid is released at a particular rate such that $\alpha=\alpha_c$, $c=1/2$ along a horizontal boundary or $c=1$ down an incline for all n, so that an identical scaling law between the extent of the flow and time is obtained regardless of the channel shape. In addition, we determine that c is a strictly decreasing function of b and that c is always greater for $H=0$ than $H=1$, when all other variables are fixed. This indicates that a higher rate of increase in the channel width leads to a slower propagation rate and that flows inside a given channel along a horizontal boundary are always slower than inside the same channel down an incline.

We found using the numerical scheme as presented in the Appendix that the dimensionless number η_N generally increases with increasing b and decreasing α for any $n>1$. A lower input rate and higher widening rate of the channel along the flow therefore leads to a lower value of c but a higher value of η_N in the expression (13). A surface plot of η_N as a function of α and b is displayed in Fig. 4 for a horizontal flow ($H=1$) inside a channel with semicircular cross section ($n=2$). In this case, η_N ranges from 0 to 1.86. Plots of η_N for different values of $n>1$ produced qualitatively similar results.

C. Squeezing fractures

We now consider viscous flows inside narrow fractures of the form $d=a|y/a|^n$, where $n<1$ so that the fluid width is much smaller than its depth. The case $n=1/2$, for instance, corresponds to the flow in between the outer surface of two identical and parallel cylinders in contact along their long axis. By the lubrication approximation, $\partial/\partial y\gg\partial/\partial z$ and the limit of Eq. (2) tends to an ordinary differential equation for u in terms of y. The solution satisfying the boundary condition $u=0$ on $z=d$ and $\partial u/\partial y=0$ on $y=0$, which follows by symmetry in y, is given by

$$u=\frac{1}{2\mu}\frac{dp}{dx}[w(z)^2-y^2], \quad (16)$$

where dp/dx is given by Eq. (3) and $2w(z)=2a|z/a|^{1/n}$ is the width of the fluid at any given height z. A thin boundary layer near the free surface $z=h$ ensures that the condition of negligible tangential stress and hence $\partial u/\partial z=0$ is satisfied at $z=h$. This boundary layer plays little role in the overall structure of the flow and does not contribute to the integral Eq. (4) in the expression for the volume flux Q to leading order.

Suppose that the length scale of the fracture is given by $a=rx^b$ for some fixed values of r and b, and note that increasing a here corresponds to the squeezing of the channel width rather than widening as for $n>1$ in Sec. II B. By substituting Eq. (16) into Eq. (4), evaluating the integral (4), and substituting them into Eq. (6), we obtain Eqs. (9) and (10) with coefficients $G=(n+1)g\sin^{1-H}\theta r^{2(1-l)}/[(n+3)\nu]$, $\bar{q}=qr^{l-1}(n+1)/(2n)$, and exponents $e_1=b(1-l)$, $e_2=1+l$, $e_3=3b(1-l)$, $e_4=1+3l$, where $l=1/n$. The position of the front is given by Eq. (13) with

$$c=\frac{n+1+\alpha(2+nH)}{n+3+H(2n+1)+b(1-n)(2-H)} \quad (17)$$

and η_N in this case depends again on α, b, n, and H. By considering the partial derivatives of Eq. (17), we find inside channels with a uniform cross section ($b=0$) that c either strictly increases or decreases for $\alpha<\alpha_c$ or $\alpha>\alpha_c$, respectively, where the critical value α_c takes the same value as what we determined for $n>1$ in Sec. II B. The value of c is constant for all n in the special case of $\alpha=\alpha_c$. Furthermore, c increases with decreasing b and attains a higher value for $H=0$ than $H=1$. This indicates that a more narrow fracture reduces the flow rate due to the frictional drag at the rigid boundaries, while a horizontal flow is always slower than a flow down an incline inside identically shaped fractures.

The dimensionless number η_N was found using the numerical scheme as presented in the Appendix to decrease with increasing α and b. A surface plot of η_N for the case of horizontal flow $H=1$ inside a fracture shape with $n=1/2$ in Fig. 5 shows that η_N ranges from 0 to 1.27, where its maximum is attained at $\alpha=b=0$. Plots of η_N for other values of $n<1$ produced qualitatively similar results.

We deduce by combining the results for $n<1$ and $n>1$ that the dividing case ($n=1$) of propagation inside a V-shaped channel, amongst all channels of the form $d=a|y/a|^n$, is fastest when the rate of increase of the total volume of fluid with time is low ($\alpha<\alpha_c$) and slowest when
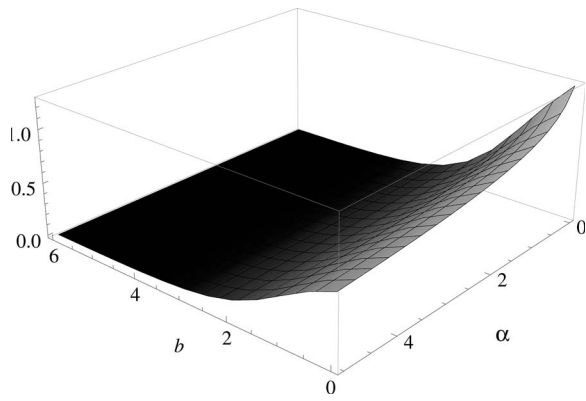
FIG. 5. Surface plot of η_N as a function of α and b in the case of horizontal flow $H=1$ with fracture shape $n=1/2$.

it is high ($\alpha > \alpha_c$). Figure 6 shows the dependence of c on n for various different values of α in the case of flows down an incline ($H=0$) with $\alpha_c=1$. Furthermore, we deduce from the representative plots in Figs. 4 and 5 that the dimensionless number η_N in Eq. (13) is higher when the temporal increase in the total volume of fluid is lower and the rate of increase of the width of a channel or fracture along the flow is higher.

D. V-shaped channels

The effect of spatial variations along the flow in the dividing case of $n=1$ can be studied by considering a V-shaped channel that is described by $d=|y|/m$, where m is the slope of the lateral walls to the plane $z=0$ and is given by $m=rx^b$ for some constants r and b. For general $b>0$, the inner vertex angle gently opens up along the direction of the flow.

The velocity profile inside V-shaped channels in any given (y,z)-plane was derived by Takagi and Huppert[9] to be

$$u = \sum_{i=0}^{\infty} \sum_{j=0}^{\infty} a_{ij} \cos \lambda_i Y \cos \lambda_j Z, \qquad (18)$$

with $\lambda_i = \pi(i+1/2)$, $Y = [(z+y/m)h^{-1} - 1]$, and $Z = [(z-y/m)h^{-1} - 1]$ being newly scaled variables and the scalar coefficients in the infinite sum are given by
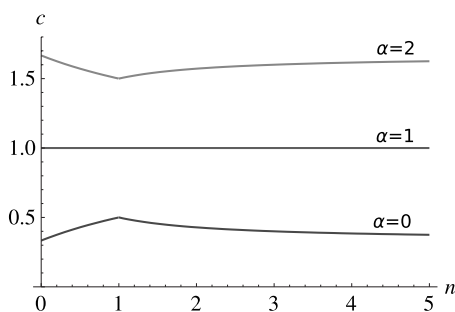

FIG. 6. A plot showing qualitatively different dependencies of c on n for different values of α when a current flows down an incline ($H=0$), in which case the critical value is given by $\alpha_c=1$. Either a maximum or minimum value of c is attained at $n=1$ for $\alpha < \alpha_c$ or $\alpha > \alpha_c$, respectively.

$$a_{ij} = \frac{(-1)^{i+j} 4m^2 h^2}{\mu(1+m^2)\lambda_i \lambda_j (\lambda_i^2 + \lambda_j^2)} \frac{dp}{dx}. \qquad (19)$$

Using this to obtain an expression for the volume flux Q and substituting it along with $A = mh^2$ into Eq. (6), we derive the evolution equation

$$m\frac{\partial h^2}{\partial t} + G\frac{\partial}{\partial x}\left[\frac{m^3}{1+m^2} h^4 \left(-\frac{\partial h}{\partial x}\right)^H \right] = 0, \qquad (20)$$

where $G \approx 0.137g\sin^{1-H}\theta/\nu$ and the global continuity equation is

$$\int_0^{x_N(t)} mh^2 dx = qt^\alpha. \qquad (21)$$

A self-similar solution can be obtained for the special case of a V-shaped channel that remains uniform in cross section throughout the flow ($b=0$), and the position of the front scales like t^c, where c does not depend on m and hence the vertex angle.[9] For general $b>0$, however, when the vertex angle varies with x, the evolution equation is not of the form (9) and generally does not admit self-similar solutions because the second term of Eq. (20) involves the term $m^3/(1+m^2)$, making it impossible to construct a similarity variable in terms of t and x. A self-similar solution only exists under conditions where the channel is either nearly flat ($m \gg 1$) or extremely narrow ($m \ll 1$) because then $m^3/(1+m^2)$ in Eq. (20) limits to m or m^3, respectively, to leading order and Eq. (20) tends to the form (9), where $e_1=b$, $e_2=2$, $e_3=b$, $e_4=4$, and $\bar{q}=q/r$ for $m \gg 1$ and $e_3=3b$ and G is adjusted by r^2 for $m \ll 1$.

The position of the front $x_N(t)$ scales like Eq. (11) and hence like t^c, where c is given by

$$c = \frac{2 + \alpha(2+H)}{4 \pm 2b + H(3+b)}, \qquad (22)$$

with the sign in the denominator positive for a V-shaped channel that is nearly flat ($m \ll 1$) or negative for a narrow V-shaped fracture ($m \gg 1$). In the limit as $m \ll 1$, c increases with b for both horizontal and inclined cases $H=1$ and $H=0$, which indicates that a gentle widening of narrow V-shaped fractures leads to a more rapid propagation rate of the flow front due to a reduction in frictional drag at the rigid walls. In the limit as $m \gg 1$, on the other hand, c decreases with b for both cases $H=0$ and $H=1$, which indicates that a gently widening V-shaped channel slows down the flow due to the constraint on the total volume. It is therefore not possible to express the position of the front in the general form t^c with constant c throughout the flow inside V-shaped channels whose sidewalls are close together initially and gradually tilt away from each other.

III. EXPERIMENTS

A series of laboratory experiments was conducted to test the theoretical results for the case of constant flux ($\alpha=1$) for a viscous fluid released in channels with uniform cross section ($b=0$). They complement the set of experimental results

obtained previously by releasing a constant volume of glycerine onto semicircular and V-shaped channels,[9] corresponding to the case of $\alpha = 0$.

The experiments were set up as follows. A 2 m long plastic gutter with a radius of curvature of 5.8 cm was braced by aluminium rods on either side and rested on a wooden base. In another set of runs, a long Perspex rectangular tank of dimensions $10 \times 15 \times 100$ cm was rotated by $45°$ about its long axis and carefully placed on orthogonal V-shaped supports, which rested on the wooden base. The wooden base was then lifted at one end or carefully levelled to the horizontal using a spirit level as required. Immediately above one end of the tank, a measuring cylinder with a nozzle diameter of 0.8 cm and a cork stopper at the base was supported, acting as a reservoir, from which pure glycerine with a density of 1.26 g cm^{-3} could be released at a constant flux onto the surfaces of interest. A typical current reached the end of the channel with a width of a few centimeters after 1–5 min, depending on the channel length and the sloping angle.

Before each run, the viscosity of the glycerine varying from 2.37 to 10.2 cm^2 s^{-1} was measured using a U-tube viscometer. A beaker filled with glycerine was poured into the cylinder up to a fixed height. The surface of the channel was carefully dried and marked every 10 cm from the point of release of fluid.

The flow of glycerine was initiated by quickly removing the cork from the cylinder. The height of glycerine inside the cylinder was kept constant throughout each run by pouring the fluid from a beaker, so that a constant flux of fluid at the point source could be maintained. The flux was determined by recording the change in mass of the beaker before and after each run, which typically lasted a few minutes. A stopclock timer was used during each run to record the time taken for the front of the flow to reach each marker on the channel surface from the point of release.

A complete set of experiments was performed with a steady flux at the source ranging from 2.4 to 6.6 cm^3 s^{-1} for each situation. Experimental data of the distance traveled by the front of the current and the time elapsed from the point of release were recorded. Figure 7 shows that the scaled experimental data with different constants of flux at the point source q, marked by different symbols, collapse nicely onto the theoretical curve in all cases for either a horizontal or inclined channel with either a semicircular or V-shaped cross section. Furthermore, no form of instability at the front was observed in any of the experiments conducted with a constant flux of viscous fluid released from a point source inside a sloping V-shaped or semicircular channel, so that the structure of the flow preserved its self-similar form. The experimental results are in good agreement with the theoretical equations in the long-time regime. The theoretical result that the extent of the flow, initiated by a constant input flux of fluid at the source ($\alpha = 1$), scales like t inside all channel shapes down an incline is supported by the agreement between the slopes of V5 and S5 in Fig. 7.
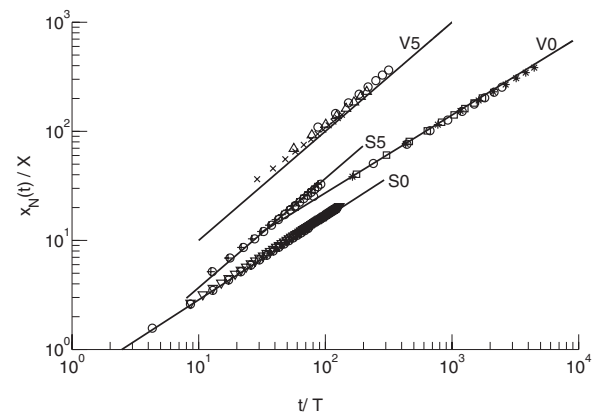

FIG. 7. Theoretical curves and experimental data for the nondimensional propagation distance of the front against nondimensional time on logarithmic axes for different channels: V-shaped on a 5°-incline (V5), horizontal V-shaped (V0), semicircular on a 5°-incline (S5), horizontal semicircular channels (S0). Different data symbols correspond to different runs with a steady flux at the source ranging from 2.4 to 6.6 cm^3 s^{-1}. The variables x_N and t have been scaled using Eq. (11) to obtain $X = (G^\alpha/\bar{q})^{1/\bar{E}}$ and $T = (G^{E_1+E_2}\bar{q}^{-E_3+E_4})^{1/\bar{E}}$ with $\bar{E} = -E_1 - E_2 + (E_3 - E_4)\alpha$ for each flow.

IV. DISCUSSION AND CONCLUSIONS

A model of unidirectional Stokes flow on rigid surfaces was used to obtain a variety of different propagation rates of viscous gravity currents, which arise by considering different releasing rates at the source inside channels that change shape down the flow. Flows inside channels of the type $d = a|y/a|^n$ evolve with a self-similar structure so that the position of the front x_N is given by Eq. (13) for some known constants c and η_N that depend on α, b, H, and n, where the total volume of fluid scales like t^α, the length scale of the channel size a like x^b with distance x from the source and $H = 0$ or $H = 1$ depending on whether the flow is inclined or horizontal, respectively. Table I shows a sample of values of c for propagation inside channels or fractures with uniform cross section ($b = 0$).

We determined that c depends linearly on α and always attains a greater value in the case of $H = 0$ than $H = 1$, when b and n are fixed. This indicates that a higher input rate of fluid at the source, and flows down an incline rather than along a horizontal channel of the same shape, always lead to a higher rate of propagation. Amongst channels that remain uniform

TABLE I. Table of values of c in the expression (13) for either horizontal or inclined flows inside various different channels; in between the outer surface of two large cylinders in contact ($n = 1/2$), inside a V-shaped channel ($n = 1$), on the inner surface of a large cylinder ($n = 2$), and inside a rectangular channel ($n \to \infty$). The cross section of the prescribed channel is uniform ($b = 0$) and the total volume of fluid scales like t^α.

	c	
n	Inclined ($H=0$)	Horizontal ($H=1$)
$1/2$	$(4\alpha+3)/7$	$(5\alpha+3)/11$
1	$(\alpha+1)/2$	$(3\alpha+2)/7$
2	$(4\alpha+3)/7$	$(2\alpha+1)/4$
∞	$(2\alpha+1)/3$	$(3\alpha+1)/5$

in cross section ($b=0$), we also found that there exists a critical value α_c such that c is either constant for all n, maximal or minimal at $n=1$, depending on whether $\alpha=\alpha_c$, $\alpha<\alpha_c$ or $\alpha>\alpha_c$, respectively. This critical value is given by $\alpha_c=1/2$ for horizontal flows and $\alpha_c=1$ for flows down an incline.

We can determine the role on the resultant flow of the volume constraint and the frictional drag at the rigid boundaries by analyzing the dependence of c on b. The theoretical results derived in Sec. II indicate that c can be expressed as a fraction of terms where b only appears in its denominator. The general trend is that increasing b, which corresponds to a gentle widening of channels or squeezing of fractures, decreases the rate of propagation of the front. This indicates that the spreading is primarily constrained by the condition on the total volume conservation inside widening channels ($n>1$), where the flow width is greater than its depth, and by frictional drag at the rigid boundaries inside squeezing fractures, where the flow width is less than its depth.

The model is useful for determining whether the resultant structure of the flow inside a given channel is governed by an equation of the form Eq. (9) and therefore self-similar. We found that currents inside channels of the type $d=a|y/a|^n$, with the length scale a varying like x^b for some non-negative constant b, have a self-similar structure and therefore the extent of the flow scales like t^c for some constant c at large times. On the other hand, flows inside channels of the type $d=|y|/m$, with m varying like x^b, have different propagation rates in the limit as $m\gg1$ or $m\ll1$. Consequently, the position of the front of any current inside narrow V-shaped fractures that gently open up and gradually tend to the limit of a completely flat surface cannot be expressed in the form t^c with constant c.

ACKNOWLEDGMENTS

APPENDIX: SELF-SIMILAR SOLUTIONS

A solution for h that satisfies Eqs. (9) and (10) is obtained as follows. By considering the scaling laws (11) and (12), it is suitable to seek a solution of the form

$$h = [G^{-E_1}\bar{q}^{-E_3}t^{\alpha E_3} - E_1]^{1/E}\phi(\eta), \tag{A1}$$

where η is a similarity variable given by

$$\eta = x/[G^{E_2}\bar{q}^{E_4}t^{E_2+\alpha E_4}]^{1/E}. \tag{A2}$$

This form allows Eq. (9) to be transformed into an ordinary differential equation given by

$$e_2\eta^{e_1}\phi^{e_2-1}[(\alpha E_3 - E_1)\phi - (E_2+\alpha E_4)\eta\phi']/E$$
$$+ [\eta^{e_3}\phi^{e_4}(-\phi')^H]' = 0 \tag{A3}$$

and Eq. (10) becomes

$$\int_0^{\eta_N} \eta^{e_1}\phi^{e_2}d\eta = 1, \tag{A4}$$

where η_N is a constant dimensionless number that is given by evaluating η in Eq. (A2) at the front of the current $x=x_N(t)$.

In the special case of releasing a constant volume of fluid at the source, which corresponds to $\alpha=0$, the differential equation (A3) reduces to the form

$$[e_2\eta^{e_1+1}\phi^{e_2} - \eta^{e_3}\phi^{e_4}(-\phi')^H]' = 0 \tag{A5}$$

and admits an analytic solution in both cases $H=0$ and $H=1$. For inclined flows ($H=0$), the first-order differential equation (A5) along with the condition that the fluid height vanishes in the long run at the source, $\phi(0)=0$, is satisfied by

$$\phi = \left(\frac{E_2}{E_4}\eta^{E_3}\right)^{1/E_4}. \tag{A6}$$

For horizontal flows ($H=1$), the second-order differential equation (A5) along with the condition (8) that the fluid height vanishes at the front of the current, $\phi(\eta_N)=0$, is satisfied by

$$\phi = \left[\frac{E_2E_4}{EE_3}(\eta_N^{E_3} - \eta^{E_3})\right]^{1/E_4}. \tag{A7}$$

The analytic solution ϕ can be substituted into Eq. (A4) to obtain an expression for η_N, which is given by either

$$[E^{E_2+E_4}/(E_2^{E_2}E_4^{E_4})]^{1/E} \tag{A8}$$

if the flow is inclined ($H=0$), or

$$\left[E_3\left[\frac{EE_3}{E_2E_4}\right]^{E_2/E_4} \Big/ B(E_1/E_3, 1+E_2/E_4)\right]^{E_4/E} \tag{A9}$$

if the flow is horizontal ($H=1$), where $B(x,y)$ is the beta function.[22]

For general $\alpha>0$, however, we must resort to a numerical method to obtain a solution $\phi(\eta)$ that satisfies Eqs. (A3) and (A4). Here, we outline a method for the horizontal case ($H=1$) so that Eq. (A3) is a nonlinear differential equation of second order. First, we rescale ϕ and η so that

$$\phi(\eta) = \eta_N^{E_3/E_4}\psi(\xi), \tag{A10}$$

where $\xi = \eta/\eta_N$ is the new similarity variable. Equations (A3) and (A4) become

$$e_2\xi^{e_1}\psi^{e_2-1}[(\alpha E_3 - E_1)\psi - (E_2+\alpha E_4)\xi\psi']/E$$
$$- [\xi^{e_3}\psi^{e_4}\psi']' = 0 \tag{A11}$$

and

$$\eta_N = \left(\int_0^1 \xi^{e_1}\psi^{e_2}d\xi\right)^{-E_4/E}. \tag{A12}$$

The leading term of the series expansion about $\xi=1$ is given by

$$\psi(\xi) \simeq [E_4(\alpha E_4 + E_2)/E]^{1/E_4}(1-\xi)^{1/E_4}, \tag{A13}$$

which is used as a starting condition in determining the numerical solution of $\psi(\xi)$. Finally, a numerical value of η_N is

determined by numerically integrating the solution using Eq. [(A12)]. Built-in MATHEMATICA functions NDSolve and NIntegrate were used to compute $\psi(\xi)$ and η_N, respectively.

[1] H. E. Huppert, J. B. Shepherd, H. Sigurdsson, and R. S. J. Sparks, "On lava dome growth, with applications to the 1979 lava extrusion of Soufriere, St. Vincent," J. Volcanol. Geotherm. Res. **14**, 199 (1982).

[2] R. W. Griffiths, "The dynamics of lava flows," Annu. Rev. Fluid Mech. **32**, 477 (2000).

[3] R. C. Kerr and J. R. Lister, "The spread of subducted lithospheric material along the mid-mantle boundary," Earth Planet. Sci. Lett. **85**, 241 (1987).

[4] R. Viskanta, "Review of three-dimensional modeling of glass melting," J. Non-Cryst. Solids **177**, 347 (1994).

[5] H. E. Huppert, "The propagation of two-dimensional and axisymmetric viscous gravity currents over a rigid horizontal surface," J. Fluid Mech. **121**, 43 (1982).

[6] H. E. Huppert, "Gravity currents: A personal review," J. Fluid Mech. **554**, 299 (2006).

[7] H. E. Huppert, "The flow and instability of viscous gravity currents down a slope," Nature (London) **300**, 427 (1982).

[8] J. R. Lister, "Viscous flows down an inclined plane from point and line sources," J. Fluid Mech. **242**, 631 (1992).

[9] D. Takagi and H. E. Huppert, "The effect of confining boundaries on viscous gravity currents," J. Fluid Mech. **577**, 495 (2007).

[10] R. C. Kerr, R. W. Griffiths, and K. V. Cashman, "Formation of channelized lava flows on an unconfined slope," J. Geophys. Res. **111**, B10206, DOI: 10.1029/2005JB004225 (2007).

[11] C. Jaupart, "Effects of compressibility on the flow of lava," Bull. Volcanol. (Heidelberg) **54**, 1 (1991).

[12] M. V. Stasiuk, C. Jaupart, and R. S. J. Sparks, "Influence of cooling on lava-flow dynamics," Geology **21**, 335 (1993).

[13] R. W. Griffiths and J. H. Fink, "Effects of surface cooling on the spreading of lava flows and domes," J. Fluid Mech. **252**, 667 (1993).

[14] C. C. Mei and M. Yuhi, "Slow flow of a Bingham fluid in a shallow channel of finite width," J. Fluid Mech. **431**, 135 (2001).

[15] M. Yuhi and C. C. Mei, "Slow spreading of a Bingham-plastic fluid on a conical surface," J. Fluid Mech. **519**, 337 (2004).

[16] J. Gratton, F. Minotti, and S. M. Mahajan, "Theory of creeping gravity currents of a non-Newtonian liquid," Phys. Rev. E **60**, 6960 (1999).

[17] C. A. Perazzo and J. Gratton, "Exact solutions for two-dimensional steady flows of a power-law liquid on an incline," Phys. Fluids **17**, 013102 (2005).

[18] J. A. Naranjo, R. S. J. Sparks, M. V. Stasiuk, H. Moreno, and G. J. Ablay, "Morphological, structural and textural variations in the 1988–1990 andesite lava of Lonquimay Volcano, Chile," Geol. Mag. **129**, 657 (1992).

[19] J. E. Bailey, A. J. L. Harris, J. Dehn, S. Calvari, and S. K. Rowland, "The changing morphology of an open lava channel on Mt. Etna," Bull. Volcanol. (Heidelberg) **68**, 497 (2006).

[20] D. J. Acheson, *Elementary Fluid Dynamics* (Oxford University Press, Oxford, 1990).

[21] G. I. Barenblatt, *Scaling, Self-Similarity, and Intermediate Asymptotics* (Cambridge University Press, Cambridge, 1996).

[22] M. Abramowitz and I. A. Stegun, *Handbook of Mathematical Functions with Formulas, Graphs, and Mathematical Tables* (Dover, New York, 1968).